Measurements of R and a Search for Heavy-Quark Production in e^+e^- Annihilation at $\sqrt{s}$ = 50 and 52 GeV

H. Sagawa,[1] T. Mori,[12] K. Abe,[1] S. Chakrabarti,[1] Y. Fujii,[1] Y. Higashi,[1] S. Ishimoto,[1] Y. Kurihara,[1] A. Maki,[1] P. Mani,[1] T. Nozaki,[1] T. Omori,[1] P. Perez,[1] Y. Sakai,[1] Y. Sugimoto,[1] Y. Takaiwa,[1] S. Terada,[1] K. Tsuchiya,[1] A. Bacala,[2] R. Imlay,[2] P. Kirk,[2] W. Marterer,[2] R. R. McNeil,[2] W. Metcalf,[2] C. P. Cheng,[3] Z. P. Mao,[3] Y. Yan,[3] Y. T. Xu,[3] H. S. Zhou,[3] Y. C. Zhu,[3] A. Abashian,[4] K. Gotow,[4] F. Kajino,[4] F. Naito,[4] F. Avignone,[5] R. Childers,[5] C. Darden,[5] J. Edwards,[5] S. Lusin,[5] C. Rosenfeld,[5] S. Wilson,[5] D. Johnson,[6] M. Frautschi,[6] H. Kagan,[6] R. Kass,[6] C. G. Trahern,[6] H. Y. Lee,[7] Winston Ko,[8] R. L. Lander,[8] K. Maeshima,[8] R. L. Malchow,[8] D. Saroff,[8] K. Sparks,[8] M. C. S. Williams,[8] A. Aldritch,[9] J. Green,[9] I. H. Park,[9] S. Sakamoto,[9] F. Sannes,[9] S. Schnetzer,[9] R. Stone,[9] S. Trentalange,[9] D. Zimmerman,[9] K. Miyano,[10] H. Miyata,[10] M. Ogawa,[10] Y. Yamashita,[11] D. Blanis,[12] A. Bodek,[12] H. Budd,[12] R. Coombes,[12] S. Eno,[12] C. A. Fry,[12] H. Harada,[12] Y. H. Ho,[12] Y. K. Kim,[12] T. Kumita,[12] S. L. Olsen,[12] R. Poling,[12] N. M. Shaw,[12] A. Sill,[12] E. H. Thorndike,[12] K. Ueno,[12] H. W. Zheng,[12] H. Asakura,[13] K. Eguchi,[13] H. Itoh,[13] S. Kobayashi,[13] A. Murakami,[13] K. Toyoshima,[13] J. S. Kang,[14] H. J. Kim,[14] S. K. Kim,[14] S. S. Myung,[14] E. J. Kim,[15] G. N. Kim,[15] D. Son,[15] H. Kozuka,[16] S. Matsumoto,[16] H. Otsuki,[16] T. Sasaki,[16] T. Takeda,[16] R. Tanaka,[16] R. Chiba,[17] K. Hanaoka,[17] S. Igarashi,[17] M. Miyashita,[17] H. Murata,[17] H. Yokota,[17] Y. Ishi,[18] T. Ishizuka,[18] T. Maruta,[18] and K. Ohta[18]

(The AMY Collaboration)

[1]*KEK, National Laboratory for High Energy Physics, Ibaraki 305*
[2]*Louisiana State University, Baton Rouge, Louisiana 70803*
[3]*Institute for High Energy Physics, Beijing*
[4]*Virginia Polytechnic Institute and State University, Blacksburg, Virginia 24061*
[5]*University of South Carolina, Columbia, South Carolina 29208*
[6]*Ohio State University, Columbus, Ohio 43210*
[7]*Chungnam National University, Daejeon 300-31*
[8]*University of California, Davis, Davis, California 95616*
[9]*Rutgers University, New Brunswick, New Jersey 08854*
[10]*Niigata University, Niigata 950-21*
[11]*Nihon Dental College, Niigata 951*
[12]*University of Rochester, Rochester, New York 14627*
[13]*Saga University, Saga 840*
[14]*Korea University, Seoul 132*
[15]*Kyungpook National University, Taegu 635*
[16]*Chuo University, Tokyo 112*
[17]*Tokyo Institute of Technology, Tokyo 152*
[18]*Saitama University, Urawa 338*

(Received 25 September 1987)

The ratio R of the cross section for e^+e^- annihilation into hadronic final states to the QED cross section for muon-pair production is measured to be $4.34 \pm 0.45 \pm 0.30$ and $4.23 \pm 0.20 \pm 0.21$ at c.m. energies of 50 and 52 GeV, respectively. From these values of R and an analysis of the event shapes we deduce a 95%-confidence-level upper limit for the production rate of new heavy charge $+\frac{2}{3}e$ or $-\frac{1}{3}e$ quarks to be 0.19 units of R.

PACS numbers: 13.65.+i, 14.40.Gx

In the quark-parton model, electron-positron annihilation into multihadronic final states proceeds by the production of pointlike quark-antiquark ($q\bar{q}$) pairs, which subsequently hadronize into physically observed particles. In its simplest version, the model predicts that the quantity R, the ratio of the cross section for annihilation into hadrons to the QED cross section for muon-pair production ($\sigma_{\mu\mu} = 4\pi\alpha^2/3s$), is $R = 3\sum e_q^2$, where the factor 3 reflects the three color states of the quarks, e_q is the quark charge in units of the electron charge, and the sum is over all quark flavors. For the five known quark flavors this predicts $R = \frac{11}{3}$. The model also predicts that the hadrons produced in an annihilation should have a structure of two back-to-back jets of particles, where the directions of the jets reflect the directions of the quarks produced in the annihilation process.

Just above the threshold for the production of particles containing new, heavy quarks Q, both R and the event-

shape distribution are expected to change significantly. Continuum production of heavy $Q\bar{Q}$ pairs increases R by an amount $R_Q = 3e_Q^2\beta(3-\beta^2)/2$, where β is the quark velocity. At energies just above the production threshold, the decays of the produced Q and $\bar{Q}$ states, which are almost at rest, result in event topologies that are nearly isotropic and quite distinct from the two-jet structure that is characteristic of light quark production.

Elaboration of the model to include QCD effects and the contribution of the virtual Z^0 raise the prediction to $R=4.1$ at $\sqrt{s}\simeq 46$ GeV,[1] the highest energy previously available (at the DESY e^+e^- storage ring PETRA), in agreement with measured values.[2,3] Also, three-jet and four-jet final states, consistent with QCD predictions for gluon radiation, are observed.[4] In spite of these modifications, measurements of R and event shapes provide sensitive tests for the existence of new quarks. The PETRA experiments used these techniques to rule out charge $+\frac{2}{3}$ and charge $-\frac{1}{3}$ quarks with masses below 23.3 and 22.7 GeV/c^2, respectively. However, some PETRA groups have reported an anomalous production rate for events containing muons,[3,5] which has been interpreted as possible evidence for the production of charge $-\frac{1}{3}$ quarks with mass $\simeq 23$ GeV.[6] We report here measurements of R and event shapes at c.m. energies of 50 and 52 GeV, made with the AMY detector at the TRISTAN e^+e^- storage ring of the Japan National Laboratory for High-Energy Physics (KEK).

The AMY detector, shown in Fig. 1, contains tracking and shower detectors located inside a 3-T solenoidal magnet coil. The charged-particle tracking detector consists of a four-layer cylindrical array of tube-type drift cells followed by a forty-layer cylindrical drift chamber (CDC) with 25 axial and 15 small-angle stereo layers.

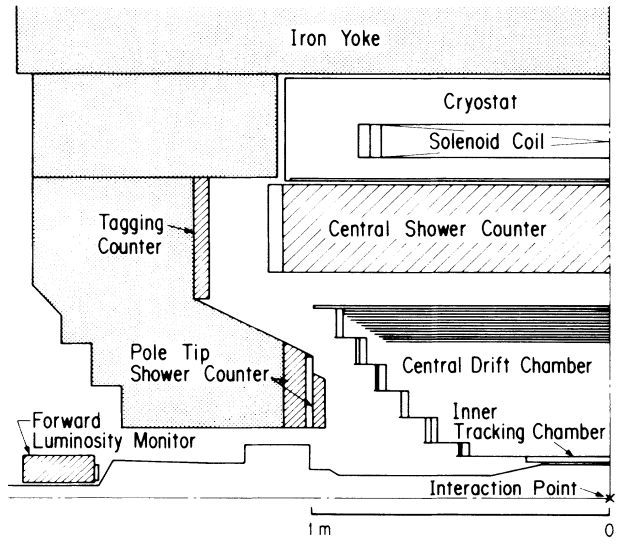

FIG. 1. Inner components of the AMY detector, showing the relative placement of the detection components. Not shown is the muon detection system, which was not used for the analysis reported here.

Charged-particle tracks are detected efficiently over the polar-angle region $|\cos\theta| < 0.87$. From Bhabha scattering events ($e^+e^- \to e^+e^-$), we determine the average spatial resolution of the CDC to be 215 μm and a momentum resolution $\Delta p_t/p_t \simeq [0.9\%\ (\mathrm{GeV}/c)^{-1}]p_t$. Radially outside of the tracking chamber, covering the region $|\cos\theta| < 0.73$, is a cylindrical electromagnetic calorimeter (SHC) of inner radius 0.79 m that consists of twenty layers of interspersed lead and resistive plastic proportional tubes. We read out azimuthally ganged signals from the anode wires for each of the twenty layers of the calorimeter. We also record the signals induced on orthogonal cathode strips, placed on either side of each proportional-tube layer. The cathode signals are ganged in radial towers with five groups spanning the depth of the SHC. Using Bhabha, $e^+e^- \to \gamma\gamma$, and $e^+e^- \to e^+e^-e^+e^-$ events, we determine an energy resolution $\sigma_E/E \simeq (35\%\ \mathrm{GeV}^{1/2})/\sqrt{E} + 1.5\%$ and a spatial resolution $\sigma_\phi \simeq 4$ mrad and $\sigma_\theta \simeq 5$ mrad. Each end-cap region contains detection elements consisting of a front and rear section of lead/scintillator calorimeter modules with an interspersed proportional-tube array for providing position measurements. Cathode-readout electrodes provided measurements of θ ($\sigma_\theta \simeq 3$ mrad) and ϕ ($\sigma_\phi \simeq 12$ mrad) in the region $15° < \theta < 26.5°$.

Bhabha events in the end caps were triggered by a front-back coincidence in either end-cap calorimeter or by a coincidence between the back sections of the calorimeters on opposite sides of the interaction region. Bhabha events in the SHC were triggered by large pulse heights in the shower counter and independently by two-track configurations in the tracking chambers. Multihadronic annihilation events were triggered by large energy pulses in the SHC or by the presence of many track segments in the tracking system. By intercomparing redundant triggers, we infer that the overall trigger efficiency for the events used for the analysis reported here is greater than 99%.

In the event reconstruction, charged tracks were required to have at least eight axial and five stereo hits that fit to a three-dimensional helix. Showers were associated with each energy cluster in the SHC that was greater than 0.2 GeV. Any shower with energy less than 1 GeV and within ± 5 cm of the extrapolated positions of a charged track was associated with that track and not treated as an independent particle.

Bhabha events were selected by the requirement of two showering particles, each with energy greater than 8 GeV, within 10° of being back-to-back collinear. In the SHC region, we distinguish Bhabha events from $e^+e^- \to \gamma\gamma$ events by requiring matching charged tracks. In the end-cap region we do not distinguish $e^+e^- \to \gamma\gamma$ events from Bhabha scattering, resulting in a contamination, which we estimate to be 1.4%,[7,8] that is subtracted off statistically. We used a Monte Carlo Bhabha-event generator that includes radiative corrections up to order α^3,[8,9] to compute the acceptance for

TABLE I. A summary of the R-value calculation at $\sqrt{s}=50$ and 52 GeV. Here N_{ev} and N_{bkg} are the number of events and the estimated number of background events, respectively; $\int L\,dt$ is the integrated luminosity; $\epsilon(1+\delta)$ is the product of the detection efficiency and the radiative correction; and $\sigma_{\mu\mu}$ is the QED cross section for $e^+e^-\to\mu^+\mu^-$. Where two errors are displayed, the first is statistical and the second is systematic.

	N_{ev}	N_{bkg}	$\int L\,dt$ (pb^{-1})	$\epsilon(1+\delta)$	$\sigma_{\mu\mu}$ (pb)	R
$\sqrt{s}=50$ GeV	95	1.9 ± 0.3	$0.69\pm0.02\pm0.03$	0.90 ± 0.04	34.7	$4.34\pm0.45\pm0.30$
$\sqrt{s}=52$ GeV	473	9.7 ± 1.2	$3.98\pm0.04\pm0.15$	0.86 ± 0.01	32.1	$4.23\pm0.20\pm0.21$

our resolution and solid-angle cuts. The calculation indicated a 2.5% contamination from $e^+e^-\to e^+e^-\gamma$ events where the final-state γ fakes an e^+ or e^- in one of the end caps. The data were corrected for this effect.

From the number of Bhabha events observed in the end caps, we determine the integrated luminosity to be $0.69\pm0.02\pm0.03$ and $3.98\pm0.04\pm0.15$ pb^{-1} at 50 and 52 GeV, respectively. Here the statistical errors are listed first, and systematic errors, corresponding to uncertainties in alignment (3.0%), position resolution (1.2%), backgrounds (0.5%), acceptance (0.6%), radiative corrections (1.1%), and detection efficiencies (1.7%) added in quadrature, are listed second. Independent determinations of the integrated luminosity for the 52-GeV sample, with use of Bhabha and $e^+e^-\to\gamma\gamma$ events in the SHC, give $4.17\pm0.10\pm0.20$ and $3.93\pm0.30\pm0.20$ pb^{-1}, respectively, results that are consistent with the end-cap measurement.

We selected multihadronic annihilation events by requiring five or more charged tracks with $|\cos\theta|\le0.85$ that originate from points within $r=2$ cm and $|z|=10$ cm of the interaction point, a total visible energy (E_{vis}) greater than half of the total c.m. energy, a momentum imbalance along the beam direction less than $0.4E_{vis}$, and more than 3 GeV energy deposited in the SHC. From the z-vertex distribution obtained with the cut on $|z|$ relaxed, we deduce the contamination from beam-gas collisions to be less than 0.2%. Monte Carlo simulations indicate that contaminations from $e^+e^-\to\tau^+\tau^-$ and two-photon processes ($e^+e^-\to e^+e^-+$hadrons) are 0.9% and 1.2%, respectively. A few of the events that pass these cuts were caused by complicated cosmic-ray showers that confused our reconstruction program. These events and one radiative Bhabha event were eliminated by a visual scan. From the way the number of selected events changes when we vary the assumed resolutions and the cut criteria, we estimate the systematic error associated with the event-selection procedure to be 2.3%.

We determine R from the relation

$$R=(N_{ev}-N_{bkg})/\epsilon(1+\delta)\int L\,dt\,\sigma_{\mu\mu}(s),$$

where N_{ev} is the number of observed multihadron annihilation events, N_{bkg} is the estimated number of background events remaining in the sample, ϵ is the detection efficiency, $1+\delta$ is a correction factor for the effects of initial-state radiation, $\int L\,dt$ is the integrated luminosity, and $\sigma_{\mu\mu}(s)$ is the QED cross section for $e^+e^-\to\mu^+\mu^-$ at the same c.m. energy. We determined ϵ and $1+\delta$ from a Monte Carlo simulation of our detector and experimental cuts. The event generator used was LUND 6.3.[10]

These numbers, summarized in Table I, give $R=4.34\pm0.45\pm0.30$ and $4.23\pm0.20\pm0.21$, at 50 and 52 GeV, respectively. The statistical error is listed first, the estimated systematic error second. In Fig. 2 we show these results together with previous measurements at lower energies.[2,3,11] Included in the figure is the standard-model prediction[12] for $\sin^2\theta_W=0.23$, $\Lambda_{\overline{MS}}=0.2$ GeV ($\overline{MS}$ denotes the modified minimal-subtraction scheme), and $m_z=92.0$ GeV/c^2. Our results are consistent with the standard-model expectation for five quark flavors; heavy-quark production with a rate in excess of 0.6 units of R is ruled out at the 95% confidence level.

The shape of the hadronic events is examined with the thrust parameter T.[13] In Fig. 3 we present the thrust

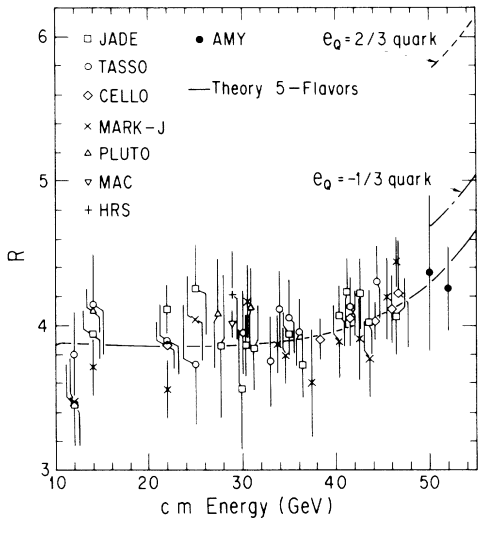

FIG. 2. Results for the measurement of R (filled circles) together with previously reported results at lower energies. The solid curve is the standard-model prediction for $\sin^2\theta_W=0.23$, $\Lambda_{\overline{MS}}=0.2$ GeV, and $m_Z=92.0$ GeV/c^2. The expected levels for new charge $+\frac{2}{3}$ quarks and charge $-\frac{1}{3}$ quarks, with the assumption of a step-function threshold factor, are shown as dashed and dash-dotted lines, respectively.

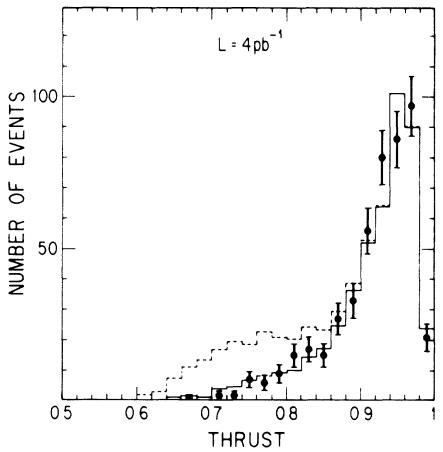

FIG. 3. Distribution of thrust values for the $\sqrt{s}=52$ GeV data and histograms showing the prediction of the LUND 6.3 Monte Carlo generator for five quark flavors (solid line) and six quark flavors (dashed line), where the sixth-flavored quark has $m_Q=25$ GeV/c^2 and a production rate corresponding to 1 unit of R.

distribution for the 52-GeV data sample. Included in the figure are histograms indicating the LUND 6.3 Monte Carlo predictions for five and six quark flavors. In the five-quark Monte Carlo simulation, two-jet events have thrust between 0.9 and 1.0; the events at lower values of thrust have additional jets caused by the radiation of gluons. The calculation of these effects is model dependent. For example, the predicted number of events with $T \leq 0.8$ is reduced by a factor of 2 if we switch to the LUND 6.2 generator.[14] For the six-quark calculation, the sixth quark is taken to have a mass $m_Q=25$ GeV/c^2 and a production rate corresponding to 1.0 unit of R. Events from heavy-quark production and decay populate the low-thrust region; 70% have $T \leq 0.8$ 23% have $T \leq 0.7$. Here, since the number of low-thrust events is primarily due to the kinematics of the decay and not the details of the dynamics, the prediction for the proportion of low-thrust events is not as strongly model dependent. Switching to the LUND 6.2 generator increases the fraction of heavy-quark events with $T \leq 0.7$ from 23% to 28%; varying m_Q from 24 to 25.5 GeV/c^2 changes the number of events below $T \leq 0.7$ by less than 10%.

The data show no indication for new-heavy-quark production. The number of events with low thrust is somewhat lower than the five-quark prediction, indicating that the LUND 6.3 generator may overestimate the number of multijet events. The six-quark version of LUND 6.3 predicts that heavy-quark production at a rate of 1.0 unit of R would result in 33 ± 4 events with $T \leq 0.7$, where the data sample has only one event. We use this to establish an upper limit for a heavy-quark production rate of 0.19 unit of R at the 95% confidence level.

Near threshold, $Q\bar{Q}$ bound states are expected to enhance the rate of pair production of sixth-flavored mesons above that predicted by these simple quark-parton model.[1] Uncertainties in these effects make the translation from cross-section limits to mass limits model dependent. A conservative approach is to use the threshold factor from the quark-parton model, in which case our cross-section limit corresponds to lower mass limits of 25.9 GeV/c^2 for $e_Q=+\frac{2}{3}$ and 23.8 GeV/c^2 for $e_Q=-\frac{1}{3}$ quarks.

We thank the TRISTAN staff for the rapid commissioning and excellent operation of the storage ring. In addition, we acknowledge the strong support and enthusiastic assistance provided by the staffs of our home institutions. This work has been supported by the Japan Ministry of Education, Science, and Culture (Monbusho), the U.S. Department of Energy and National Science Foundation, the Korean Science and Engineering Foundation and Ministry of Education, and the Academia Sinica of the People's Republic of China.

[1]T. Appelquist and H. D. Politzer, Phys. Rev. D **12**, 1404 (1975); M. Dine and J. Sapirstein, Phys. Rev. Lett. **43**, 668 (1979); K. G. Chetyrkin *et al.*, Phys. Lett. **85B**, 277 (1979); W. Celmaster and R. J. Gonsalves, Phys. Rev. Lett. **44**, 560 (1980); J. Jersak, E. Laermann, and P. M. Zerwas, Phys. Rev. D **25**, 1218 (1982); S. Gusken *et al.*, Phys. Lett. **155B**, 277 (1985).

[2]W. Bartel *et al.*, Phys. Lett. **160B**, 337 (1985); M. Althoff *et al.*, Phys. Lett. **138B**, 441 (1983); H.-J. Behrend *et al.*, Phys. Lett. **144B**, 297 (1984); H.-J. Behrend *et al.*, Phys. Lett. B **183**, 400 (1987).

[3]B. Adeva *et al.*, Phys. Rev. D **34**, 681 (1986).

[4]R. Brandelik *et al.*, Phys. Lett. **86B**, 243 (1979); D. P. Barber *et al.*, Phys. Rev. Lett. **43**, 830 (1979); Ch. Berger *et al.*, Phys. Lett. **86B**, 418 (1979); W. Bartel *et al.*, Phys. Lett. **91B**, 142 (1980); W. Bartel *et al.*, Phys. Lett. **115B**, 338 (1982).

[5]W. Bartel *et al.*, Z. Phys. C **36**, 15 (1987).

[6]F. Cornet *et al.*, Phys. Lett. B **174**, 224 (1986); V. Barger, R. J. N. Phillips, and A. Soni, Phys. Rev. Lett. **57**, 1518 (1986).

[7]J. Fujimoto, M. Igarashi, and Y. Shimizu, Prog. Theor. Phys. **77**, 118 (1987).

[8]S. Kawabata, Comput. Phys. Commun. **41**, 127 (1986).

[9]K. Tobimatsu and Y. Shimizu, Prog. Theor. Phys. **74**, 567 (1985).

[10]T. Sjostrand and M. Bengtsson, Comput. Phys. Commun. **43**, 367 (1987).

[11]W. Bartel *et al.*, Phys. Lett. **129B**, 145 (1983); B. Adeva *et al.*, Phys. Rev. Lett. **50**, 799 (1983); R. Brandelik *et al.*, Phys. Lett. **113B**, 499 (1982); E. Fernandez *et al.*, Phys. Rev. D **31**, 1537 (1983); D. Bender *et al.*, Phys. Rev. D **31**, 1 (1983); L. Criegee and G. Knies, Phys. Rep. **83**, 153 (1982).

[12]For the standard-model curve, we use the formalism of Ref. 1 together with results for $\sin^2\theta_W$, $\Lambda_{\overline{MS}}$, and m_Z given by U. Almadi *et al.*, Phys. Rev. D **36**, 1385 (1987); K. Varvell *et al.*, Z. Phys. C **36**, 1 (1987); A. Benvenuti *et al.*, Phys. Lett. B **195**, 97 (1987).

[13]E. Farhi, Phys. Rev. Lett. **39**, 1587 (1977).

[14]T. Sjostrand, Comput. Phys. Commun. **39**, 347 (1986).

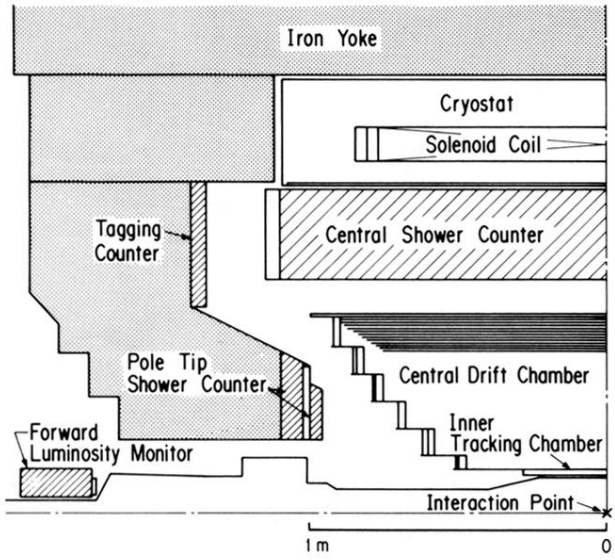

FIG. 1. Inner components of the AMY detector, showing the relative placement of the detection components. Not shown is the muon detection system, which was not used for the analysis reported here.